DOE/MC/29061-96/C0661 CONF-9510109--39

Life Prediction of Advanced Materials for Gas Turbine Application

Author:

Sam Y. Zamrik
Asok Ray
Donald A. Koss

Contractor:

South Carolina Energy Research and Development Center
Clemson University
Clemson, SC 29634

Contract Number:

DE-FC21-92MC29061
Subcontract No. AGTSR 9301SR012D

Conference Title:

Advanced Turbine Systems Annual Program Review

Conference Location:

Morgantown, West Virginia

Conference Dates:

October 17-19, 1995

Conference Sponsor:

U.S. Department of Energy, Office of Power Systems Technology,
Morgantown Energy Technology Center

Contracting Officer Representative (COR):

Norman Holcombe

DLC

Disclaimer

Available to DOE and DOE contractors from the Office of Scientific and Technical Information, 175 Oak Ridge Turnpike, Oak Ridge, TN 37831; prices available at (615) 576-8401.

Available to the public from the National Technical Information Service, U.S. Department of Commerce, 5285 Port Royal Road, Springfield, VA 22161; phone orders accepted at (703) 487-4650.

P6

Life Prediction of Advanced Materials for Gas Turbine Application

Dr. Sam Y. Zamrik (SYZESM@engr.psu.edu; 814-865-5241)
Dr. Asok Ray (A2R@ecl.psu.edu; 814-865-6377)
Dr. Donald A. Koss (Koss@ems.psu.edu ; 814-865-5447)
The Pennsylvania State University
121 Hammond Bldg.
University Park, Pa 16802

Introduction

Most of the studies on the low cycle fatigue life prediction have been reported under isothermal conditions where the deformation of the material is strain dependent. In the development of gas turbines, components such as blades and vanes are exposed to temperature variations in addition to strain cycling. As a result, the deformation process becomes temperature and strain dependent. Therefore, the life of the component becomes sensitive to temperature-strain cycling which produces a process known as "thermomechanical fatigue, or TMF". The TMF fatigue failure phenomenon has been modeled using conventional fatigue life prediction methods, which are not sufficiently accurate to quantitatively establish an allowable design procedure. To add to the complexity of TMF life prediction, blade and vane substrates are normally coated with aluminide, overlay or thermal barrier type coatings (TBC) where the durability of the component is dominated by the coating/substrate constitutive response and by the fatigue behavior of the coating. A number of issues arise from TMF depending on the type of temperature/strain phase cycle:

1- time-dependent inelastic behavior can significantly affect the stress response. For example, creep relaxation during a tensile or compressive loading at elevated temperatures leads to a progressive increase in the mean stress level under cyclic loading.

2- the mismatch in elastic and thermal expansion properties between the coating and the substrate can lead to significant deviations in the coating stress levels due to changes in the elastic modulii.

3- the "dry" corrosion resistance coatings applied to the substrate may act as primary crack initiation sites.

Crack initiation in the coating is a function of the coating composition, its mechanical properties, creep relaxation behavior, thermal strain range and the strain/temperature phase relationship. Of particular importance are the coating ductility and the coefficient of thermal expansion mismatch between the coating and substrate, which can cause thermally induced strains causing cracking at the surface and creep relaxation.

As a result of the complex constitutive behavior of the coating/substrate system, TMF life prediction methodology has yet to be developed to explicitly describe the fatigue response of the coating/substrate systems.

Objectives

The main focus of the research program is directed towards life prediction modeling of coated advanced gas turbine materials. Emphasis is placed on life characterization which is based on low cycle

Research sponsored by U.S Department of Energy's Morgantown Energy Technology Center, under cooperative agreement DE-FC21-92MC29061 with the South Carolina Energy Research and Development Center, subcontract AGTSR 9301SR012D

fatigue (LCF) under isothermal conditions and also on thermo-mechanical fatigue (TMF). The microstructure of failed coated and uncoated specimens is being analyzed to assess the deformation response, the fracture mechanism, and the environmental effect. IN 738 LC has been selected as a basic material which will be followed in the future by directionally solidified (DS) and single crystal (SC) materials..

Project Description

The project is divided into two parts: experimental and analytical. The TMF experimental part is not as simple as the isothermal fatigue testing and becomes very sensitive to temperature/strain programming. Software programs for TMF and heating were developed to cover the following loading schemes:

-Strain-temperature out-of-phase cycling where the strain is in compression at the maximum temperature.

-Strain-temperature out-of-phase cycling where the strain is held in compression for a period of 90 seconds at the maximum temperature. This type of cycling simulates the creep and relaxation effects and introduces the mean stress.

The experimental facility consists of servo-hydraulic MTS system designed for axial-torsion strain cycling at high temperatures. Only the axial load component was used. The specimen was heated by induction with three adjustable coils to maintain uniform temperature distribution over the gage length with five thermocouples equally spaced and wrapped around the gage length measuring the temperature distribution. Strain was measured by an axial high temperature air cooled MTS extensometer with wedge probes placed over one inch gage length. The strain and temperature input were computer controlled. The TMF test system is shown in Fig. 1. Thermocouples and coils placement on the specimen are shown in Fig. 2.

Analytical And Experimental Approach

a- Analytical Solution:

Life Prediction Model Development:

In developing a life prediction model, the specimens are subjected to mechanical and thermal loads in addition to the environmental effect which has to be incorporated in the analysis. Most of the current life models under constant temperature (isothermal) conditions utilize a simple approach using total or plastic strain range-cycle relation such as the Coffin-Manson relation. The plastic strain range is selected at the mid-life cycle range which describes the average deformation process in fatigue cycling. However, this type of approach is not adequate to describe the life under the variable temperature and strain since the damage process is dependent on strain, mean stress, thermal effect, creep and ductility. The life prediction model has to incorporate all these variables and since cyclic strain is the primary mechanical driving mechanism, the mid-life strain-cycle as represented by the hysteresis loop is incorporated in a proposed damage model based on the concept of "non-linear continuum damage mechanics". The continuum damage model is a strain base and to accurately predict the mid-life strain-cycle hysteresis loop, a viscoplastic model proposed by A. Freed (1) is used. The viscoplastic model can also accounts for the material response to kinematic or isotropic hardening. These two processes effects the yield phenomenon . During kinematic hardening the center of the yield surface moves gradually while the radius of the yield surface remains constant in a stress space, as a result a mean stress develops. For the isotropic hardening case, the center of the yield surface remains fixed in the stress space while the radius of the yield surface progressively increases resulting in a decrease in the hysteresis loop width. The two types of hardening mechanisms are shown in Figs. 3 and 4.

Viscoplastic Model

The life prediction model under development has two components: a viscoplastic component and a non-linear continuum damage component. The vsicoplastic component has been completed and is presented in a simplified form. The model accounts for the nonlinear kinematic hardening process observed in IN 738 LC material under a TMF compressive and hold-time strain cycling. The two type of cycle produces a significant mean stress.

The basic components of the model is strain, strain rate, stress, temperature, and creep rate. For an isothermal uniaxial LCF strain cycle, the total strain is:

$$\varepsilon = \varepsilon_e + \varepsilon_{in}$$

and the rate:

$$\dot{\varepsilon} = \dot{\varepsilon}_e + \dot{\varepsilon}_{in}$$

the inelastic strain rate is also a function of deviatoric stress S, internal stress variables κ and temperature T:

$$\dot{\varepsilon}_{in} = f(S, \kappa, T)$$

Three internal stress variables, which are represented by κ, characterize the inelastic deformation of the material : the time dependent back stress B which takes into account the kinematic hardening; the time dependent drag stress D, a scalar quantity, which measures the isotropic hardening; and the time dependent limiting stress L, which is also a scalar quantity, accounts for the radius of the yield surface. The model is a rate process and uses the concept of an effective stress Σ, sometimes referred to as "overstress", which is responsible for the yield process.

The deviatoric stress S for uniaxial stress is defined as:

$$S = \frac{2}{3}\sigma_x$$

and the effective stress for the uniaxial case is defined as:

$$\Sigma_x = S_x - B_x$$

For steady state conditions under varying temperatures when the hysteresis loop is saturated, the internal stresses are written for the uniaxial case as a rate in the form of :

$$\dot{B}_x = H_b\,(\dot{\varepsilon}^p_x - \frac{B_x}{L}\dot{\varepsilon}^p_x) + \frac{B_x}{H_b}\frac{\partial H_b}{\partial T}\dot{T}$$

and

$$\dot{L} = \frac{L}{H_L}\frac{\partial H_L}{\partial T}\dot{T}$$

$$\dot{D} = \frac{D}{H_d}\frac{\partial H_d}{\partial T}\dot{T}$$

where H_b is the kinematic modulus and H_L, H_d are the isotropic hardening modulii. At the steady state condition, the back stress saturates, i.e. $\dot{B}_x = 0$. In addition, if the temperature T is constant, i.e., $\dot{T} = 0$, the scalar variables L and D become constants.

The inelastic strain rate is expressed as:

$$\dot{\varepsilon}_{in} = \theta\; Z(\zeta)\frac{\Sigma_x}{\Sigma_2}$$

where the thermal diffusivity, θ , is defined as:

$$\theta = \left\{\exp\left[\frac{-Q}{kT}\right]\right\} \quad \text{for } T \geq T_m/2$$

$$\theta = \left\{\exp\left[\frac{-2Q}{kT_m}\left\{\ln\left(\frac{T_m}{2T}\right) + 1\right\}\right]\right\}$$

for $T \leq T_m/2$

and

$$\Sigma_2 = \sqrt{\frac{2}{3}\Sigma_{ij}\Sigma_{ij}}$$

and for the uniaxial case, becomes $\Sigma_2 = |\,\Sigma_x\,|$

The Zener Holloman parameter Z is defined as:

$$Z(\zeta) = A\,\zeta^{\,n} \qquad \text{if } \zeta \le 1$$

$$Z(\zeta) = A\,e^{\,n(\zeta - 1)} \qquad \text{if } \zeta > 1$$

where A and n are material constants and ζ is defined at the steady state condition and at mid-life as:

$$\zeta = \frac{|\Sigma_x|}{D}$$

$\Sigma_x = S_x - B_x$ and D becomes a constant for the isothermal case but varies for TMF conditions.

Under steady state or during a stabilized cycle, the inelastic strain rate can be assumed to approach the steady state creep rate $\dot{\varepsilon}_{ss}$. Having steady state creep rate data at several temperatures and stress levels, the Zener-Holloman stress function $Z(\zeta) = \frac{\dot{\varepsilon}_{ss}}{\theta}$ is plotted vs. the deviatoric stress S as shown in Fig. 5. From Fig. 5, C is the point where the curve deviates from a linear relation, n is the slope of the linear section and A is the intercept or for a better accuracy, a least square curve fit can be used.

The kinematic hardening modulus H_b and the isotropic hardening modulii H_L, H_d are determined by an optimization process using stabilized LCF hysteresis loop generated at three constant temperatures (mid-life loops). Once these parameters are determined, the TMF inelastic strain-cycles are predicted from isothermal inelastic-strain cycles for any cyclic strain range with or without hold-time (creep) as shown in Figs. 6-8.

b- Experimental Approach:

Material And Test Results

- Material, Specimen and Coatings:

The nickel base superalloy IN 738 LC material, solution-treated condition (1120°C for 2 hrs, air cooled), was received in the as-cast bars having one inch (25.4mm) in diameter by six and quarter inches (16 cm) in length. Tubular test specimens machined by a low stress grind process were aged in a dynamic vacuum of ~ 2.7×10^{-4} pa. for 24 hrs at 843°C (1550°F) followed by an air cool. The microstructure of the cast material consists of dentritic structure with a high volume fraction of fine-scale gamma-prime particles as well as large second phase particles, mostly primary gamma prime and/or carbides, in the interdendritic regions. No evidence of large-scale (>1mm) porosity was seen. The chemical composition of the material is presented in Table 1. Fatigue specimens were overlay coated (NiCoCrAly) over either three quarter or full length of the gage length where the gage length was one inch. The overlay coating thickness was 5.8 mil (147 μm) and was deposited on the specimen using a low pressure plasma spraying process. The N_iAl-based aluminide coating was deposited using a pack cementation process and had a thickness of 1.3 mil (33 μm) with a 0.4 mil (10 μm) deep diffusion zone.

- Tests Results:

1- <u>Isothermal Fatigue Tests (Uncoated Specimens)</u>

A total of six isothermal fatigue tests were conducted at 1500°F under different strain range amplitudes: three of these were LCF with two under a compressive hold-time and one under a tensile-hold time of 90 seconds. The difference between the tension and compression 90 seconds hold-time tests is the apparent response of the mean stress. In the tension test, the mean stress became compressive, while in the compression test, it became tensile. A comparison of lives between the two types of tests at 0.5% strain range showed that the compressive hold test reduced the life by a factor of 5 as a result of the tensile mean stress which develops.

At 1600°F, one 90-second hold-time compressive test was completed at a strain range of 0.5%. The fatigue life (N_i) was 303 cycles as compared to a similar hold-time test at 1500°F where the fatigue life was 517 cycles. The 100°F temperature increase reduced the life by 41%. N_i is defined as the cycle at which the peak tensile stress begins to decrease rapidly during strain cycling.

2- Isothermal Fatigue Tests (Overlay Coated Specimens)

At 1600°F, one 90-second hold-time compressive test was conducted at a strain range of 0.5%. The fatigue life ($N_i = 613$) for the coated specimen was longer when compared to a similar uncoated hold-time test at the same strain range and temperature ($N_i = 135$).

3- Thermomechanical Fatigue Tests (TMF) (Uncoated Specimens)

At 1600°-900°F, a total of five TMF tests were completed. The first two TMF tests were conducted at strain ranges of 0.5% and 0.8% and the next three TMF tests with compressive hold-time of 90 seconds at the same strain ranges. A comparison of life, at strain range of 0.5%, between the TMF (zero hold-time) tests at 1600°-900°F and TMF with 90 seconds hold time in compression, showed a significant reduction in life. For example, at a strain range of 0.5%, the N_i life of 790 cycles was reduced by the hold time test to 563 cycles while at 0.8% strain range the life was reduced from 282 cycles to 112 cycles.

4- Thermomechanical Fatigue Tests (TMF) (Overlay Coated Specimens)

The one in. gauge lengths of the IN 738LC specimens were either partially coated to 3/4 in. or to full length of the specimen. The overlay coating thickness was 5.8 mil (147 μm). Two - 3/4 in gauge length coated specimens were tested at 1600°-900°F without creep effect (zero hold time) at strain ranges of 0.5% and 0.8% and one test was at 0.8% strain range with compressive hold-time of 90 seconds at the maximum temperature. Specimen failure occurred by cracking either outside the coated section or at the transition region between coated and uncoated sections of the specimen. As a result, fatigue lives are not reported here.

The fully coated specimens were tested at a strain range of 0.5% without and with 90 seconds compression hold-time. For the TMF tests (zero hold-time), the overlay coating improved the life of the uncoated substrate from 790 cycles to 2058 cycles. However, introducing hold-time, the overlay life was reduced substantially from 2058 cycle to 643 cycles .

5- Thermomechanical Fatigue Tests (TMF) (Aluminide Coated Specimens)

Four TMF fatigue tests were conducted on aluminide coated specimens. Three tests with zero hold-time at strain ranges of 0.3%, 0.5% and 0.8% and one test with 90-seconds compressive hold-time at 0.5% strain range. The aluminide coating reduced the fatigue life as compared to uncoated specimens by a factor of 2.2 for the 0.5% strain range tests and by 3.6 for the hold-time test. TMF test data for the two types of coatings are shown in Fig. 9 and Table 2 is a summary of all fatigue tests completed to date.

Microstructure Failure Observations of Tested Specimens:

i- Uncoated Specimens: Crack Initiation Behavior

Crack initiation and propagation was transgranular under all test conditions. Optical and scanning electron microscopy revealed that crack initiation occurred at both the outer and inner walls as shown in Fig. 10. The fracture surfaces near the crack initiation sites were flat, semi-circular and oxidized.

The isothermal fatigue test specimens all exhibited fatigue crack initiation predominantly from the outer surface. In contrast, the TMF specimens often contained both an outer initiation along with numerous small cracks initiating on the interior of the specimen.

ii- Overlay Coated Specimen: Crack Initiation Behavior

Three overlay coated specimens have been tested in fatigue under both isothermal and TMF conditions (see Table 2). The isothermal test at the strain range of 0.5%, that included a hold time of 90-seconds in compression, had multiple crack initiations on the uncoated interior surface of the specimen. However, the TMF cycling initiated many small surface cracks in the coating as shown in Fig. 11. A few cracks propagated through the coating and penetrated the substrate (Fig. 12) but most were confined to the coating (Fig. 13). Also debonding of the overlay coating was observed in the TMF type tests which was absent in isothermal tests.

iii- Aluminide Coated Specimen: Crack Initiation Behavior

Four fatigue specimens were aluminide coated over three quarter of one inch gauge length. Three specimens were tested with no hold-time and one where the compressive strain was held for 90 seconds at maximum temperature. TMF test results showed that the cracks initiated in the coating, propagated through the inter-diffusion zone and penetrated the substrate as shown in Figs. 14 and 15. The aluminide coating showed both intergranular and transgranular fracture features. Fig. 16 shows the aluminide coating structure.

Future Work

TMF tests of coated specimens will continue to compliment the analytical approach. The effect of coating on life will be characterized by microstructural analysis which will describe the deformation and fracture mechanisms. Other types of material's structures such as DS and SC materials and other types of coatings will be investigated in the future where life is affected by the material durability and resistance to creep damage.

Industrial Partners Participation

The PI of the research program is in direct consultation with our industrial partners: Westinghouse Electric, Power Generation Division in Orlando, Fl., Allied Signal Aerospace Co. of Phoenix, AZ and Solar Turbine of San Diego, California..

Acknowledgment

The authors would like to acknowledge the research support by U.S Department of Energy's Morgantown Energy Technology Center, under cooperative agreement DE-FC21-92MC29061 with the South Carolina Energy Research and Development Center. The program is under subcontract AGTSR 9301SR012D. The research program is supporting two doctoral candidates: Messrs. Ravindra Annigeri and Mark Renauld.

Also our gratitude to Mr John Junkin of Westinghouse, Power Division, Orlando, Florida, for his support in providing the overlay coating on the specimens and to Dr Graham Webb of Allied Signal Aerospace Co. of Phoenix, Arizona, for his contribution in coating specimens with aluminide coating.

References

1- Freed, A., "Thermoviscoplastic Model with Application to Copper," NASA Technical Paper 2845,1988.

2- Kuwabara, Nitta, A., and T. Kitamura, "Thermal-Mechanical Fatigue Life Prediction In High Temperature Component Materials For Power Plant," ASME Int. Conf. on Advances in Life Prediction Methods, Materials Conference, N.Y., 1983, pp. 131-141.

3- Au, P., and R. V. Dainty, "Isothermal Low Cycle Fatigue Properties of Diffusion Aluminide Coated Nickel and Cobalt Based Superalloys," Surface Modification Technologies III, Eds., T.S.Sudarshan and D. G. Bhat, TMS, 1990, pp.729-747.

4- Ostergren, N., J., " A Damage Function and Associated Failure Equations for Predicting Hold-Time and Frequency Effects in Elevated Temperature, Low Cycle Fatigue," Journal of Testing and Evaluation, Vol. 4, No. 5, Sept. 1976, pp. 327-339.

5- Jiao, F. " Low Cycle Fatigue Behavior of IN 738 LC at 1223K," Proc. of Third Int. Conf. on Low Cycle Fatigue and Elasto-Plastic Behavior of Materials," 1992, pp.298-303.

6- Strang, S., "High Temperature Properties of Coated Superalloys," Behavior of High Temperature Alloys in Aggressive Environment, Proc. of Petten Int. Conf., The Metal Society of London, 1979, pp.595-611.

7- Castillo, R.and A. K. Koul, "Effects of Microstructure Instability on the Creep and Fracture Behavior of Cast IN 738 LC Ni-base Superalloy," High Temperature Alloys for Gas Turbines and Applications," Betz, W., eds, D. Reidel Publishing Co., Dordrecht, 1986, pp.1395-1409.

8- Castillo, R.and A. K. Koul, "Factors Influencing the Residual Creep Life Prediction of Service Exposed Ni-base Superalloys Components," Life Assessment and Repair Technology for Combustion Turbine Hot Section Components, ASM Int., Metal Park, 1990, pp 19-34.

9- Tipler, H., R., "Regeneration of the Creep Properties of a Cast Ni-Cr-base Alloy," AGARD-CP-317, Paper #12.

10- Castillo, R., A. K. Koul and E. H. Toscano, "Lifetime Prediction under Constant Load Creep Conditions for a Cast Ni-base Superalloy," Journal of Engineering for Gas Turbines and Power, vol. 109, 1987, pp.99-106.

11- Kloos, K., H., J. Granacher, and H. Demus, "Creep Rupture Strength of Cast Turbine Blades under Hot Gas Corrosion," Corrosion and Mechanical Stress at High Temperature, Guttmann, V. and Merz, M. eds., Applied Science Publishers, London, 1981, pp. 243-255

12- Hartnagel, W., R. Bauer and H. W. Grunling, "Constant Strain Rate Creep Tests with Gas Turbine Blade Material under Hot Corrosion Environmental Conditions," Corrosion and Mechanical Stress at High Temperature, Guttmann, V. and Merz, M. eds., Applied Science Publishers, London, 1981, pp. 257-272.

13- Villat, M., P. Felix., "High Temperature Corrosion Protective Coating for Gas Turbines," Sulzer Technical Review, Vol. 3, 1976, pp. 97-104.

14- Nazmi, M. Y., "High Temperature Low Cycle Fatigue of IN 738 and Application of Strain Range Partitioning," Metallurgical Trans. A, ASM, Vol. 14A, March 1983, pp. 449-461.

15- Zamrik, S. Y.," An Interpretation of Axial Creep-Fatigue Damage Interaction in Type 316 Stainless Steel," ASME Trans., Journal of Pressure Vessel Technology, Vol.112, Feb. 1990, pp. 4-19.

16 Gabrielli, F, M. Marchionni and G. Onofrio, "Time Dependent Effect on High Temperature Low Cycle Fatigue and Fatigue Crack Growth Propagation of Nickel Base Superalloys," Advances in Fracture Research, Proc., of the 7th Int. Conf. on Fracture (ICF7), March 1989, pp. 1149-1163.

TABLE 1: CHEMICAL COMPOSITION OF ALLOY IN 738 - LC

Heat Treatmeant	Element	Percentage
Solutionize at 2050 °F(1120 °C) for 2 hr followed by aging at 1550 °F (843 °C) for 24 hr.	Cr	15.7 - 16.3
	Co	8.0 - 9.0
	Ti	3.2 - 3.7
	Al	3.2 - 3.7
	W	2.4 - 2.8
	Mo	1.5 - 2.0
	Ta	1.5 - 2.0
	Nb	0.6 - 1.1
	Ni	Balance

Table 2. Penn State IN-738LC Fatigue Test Summary

Specimen #	Coating	Emech	ISO/TMF	Temp Range F (C)	Hold Time Seconds	Cycles				Mid-Cycle	Peak Stress (MPa)	Valley Stress (MPa)	Mean Stress (MPa)
						Ni	N90	N70	N50				
20	-	0.3%	ISO	1500 (816)	0		86759 (runout)			43561	247	-184	31.5
11	-	0.5%	ISO	1500 (816)	0	2494	3189	3476	3807	1500	420	-343	38.5
17	-	2.0%	ISO	1500 (816)	0		Spec Separation, N=5			3	757	-820	-32
16	-	0.5%	ISO	1500 (816)	90 s (T)	4611	4959	5128		2467	220	-483	-132
22	-	0.3%	ISO	1500 (816)	90 s (C)	8312	8542	8648	8731	4239	362	-80	141
21	-	0.5%	ISO	1500 (816)	90 s (C)	517	622	649	670	225	487	-224	132
25	-	0.5%	OP TMF	900-1500 (482-816)	0	5177	5427	5444	5458	2661	507	-209	149
27	-	0.7%	OP TMF	900-1500 (482-816)	0	847	1253	1361	1497	582	656	-371	143
28	-	0.5%	IP TMF	900-1500 (482-816)	0		10012 (runout)			5052	199	-530	-166
31*	-	0.5%	ISO	1600 (871)	90 s (C)	135	250	285	324	146	397	-200	98.5
36	-	0.5%	ISO	1600 (871)	90 s (C)	303	481	508	526	250	448	-204	122
29	-	0.5%	OP TMF	900-1600 (482-871)	0	790	1139	1147	1154	562	623	-189	217
32	-	0.8%	OP TMF	900-1600 (482-871)	0	282	Spec Separation, N=329			175	716	-400	158
35	-	0.3%	OP TMF	900-1600 (482-871)	90 s (C)	6387	6924	7371			456	9	233
33	-	0.5%	OP TMF	900-1600 (482-871)	90 s (C)	563	Spec Separation, N=642			258	608	-194	207
38	-	0.5%	OP TMF	900-1600 (482-871)	90 s (C)	785	1113	1165	1226	405	565	-170	198
34	-	0.8%	OP TMF	900-1600 (482-871)	90 s (C)	112	Spec Separation, N=117			39	720	-398	161
13	Overlay	0.5%	ISO	1600 (871)	90 s (C)	613	786	817	835	420	430	-210	110
12	Overlay	0.5%	OP TMF	900-1600 (482-871)	0	1171	1543	(fractured)		789	636	-201	218
14	Overlay	0.8%	OP TMF	900-1600 (482-871)	0	172	Spec Separation, N=173			92	797	-412	193
15	Overlay	0.8%	OP TMF	900-1600 (482-871)	90 s (C)	55	Spec Separation, N=66			22	794	-392	201
41	Overlay	0.5%	OP TMF	900-1600 (482-871)	0	2058	2371	2373	2376	1102	581	-160	211
50	Overlay	0.5%	OP TMF	900-1600 (482-871)	90 s (C)	643	1010	1078	1126	350	578	-160	209
2	Aluminide	0.3%	OP TMF	900-1600 (482-871)	0	6540	7876	8161	8598	3958	432	-26	203
4	Aluminide	0.4%	OP TMF	900-1600 (482-871)	0	1356	1754	1826	1880	753	451	-149	151
1	Aluminide	0.5%	OP TMF	900-1600 (482-871)	0	360	547	609	678	245	523	-271	126
7	Aluminide	0.8%	OP TMF	900-1600 (482-871)	0	190	Spec Separation, N=239			113	555	-393	81
8	Aluminide	0.5%	OP TMF	900-1600 (482-871)	90 s (C)	218	456	472	483	100	529	-235	147

Ni=Cycle for which a deviation from maximum linear tensile stress was first detected

N90=Number of cycles to 90% of maximum linear tensile stress; 10% load drop

N70=Number of cycles to 70% of maximum linear tensile stress; 30% load drop

N50=Number of cycles to 50% of maximum linear tensile stress; 50% load drop

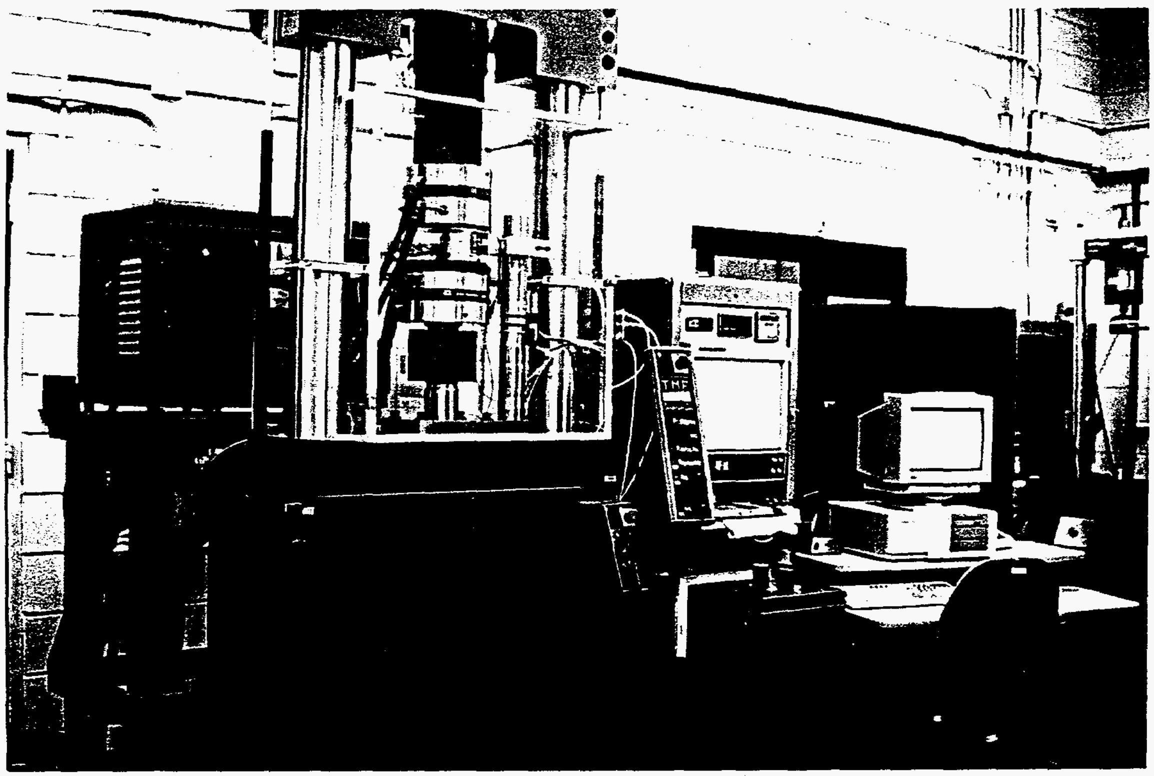

Figure 1. Computer controlled test system for thermomechanical fatigue test

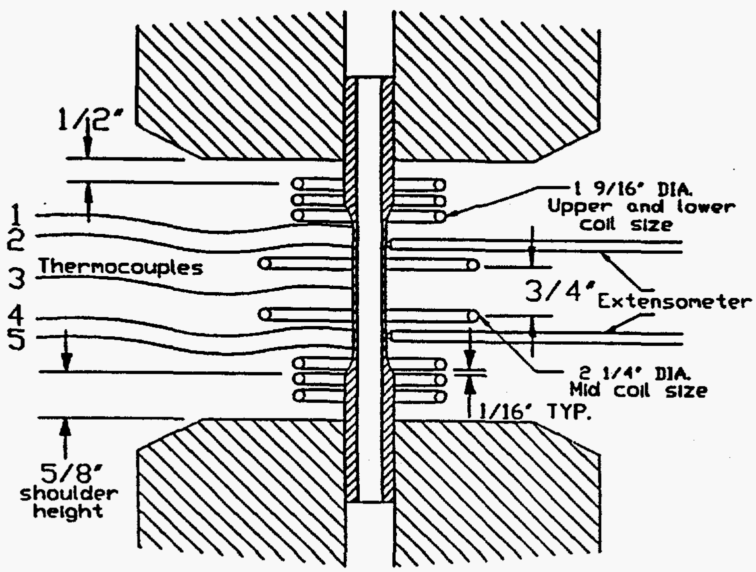

Figure 2. Cross-section of specimen, induction coils and thermocouples

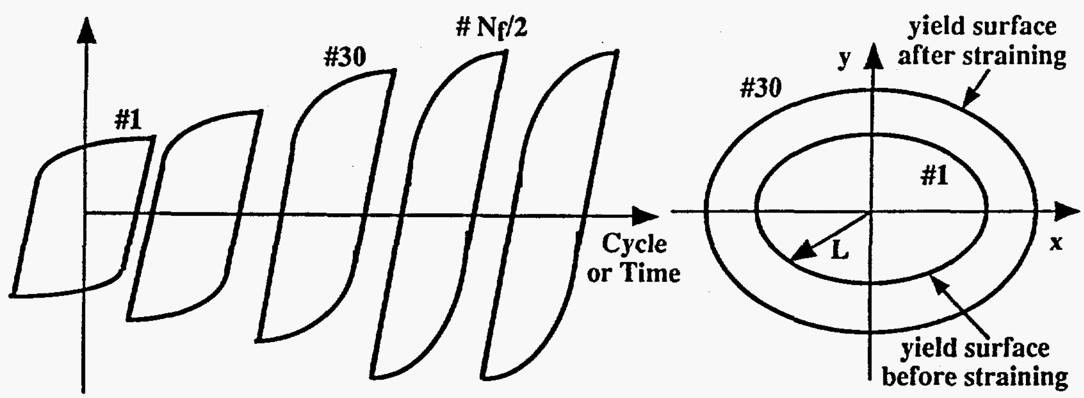

Figure 3. Isotropic hardening behavior in polycrystalline materials

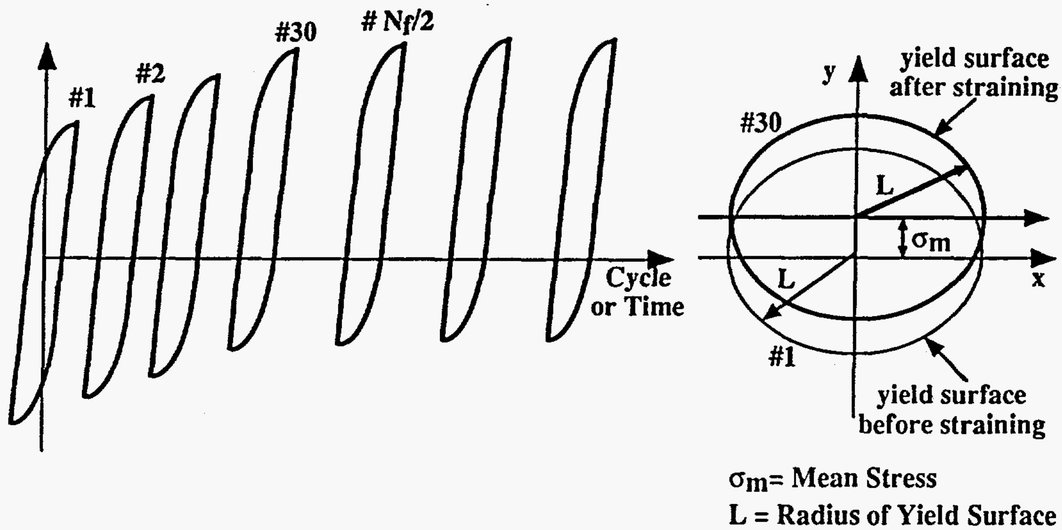

Figure 4. Kinematic hardening behavior in polycrystalline materials

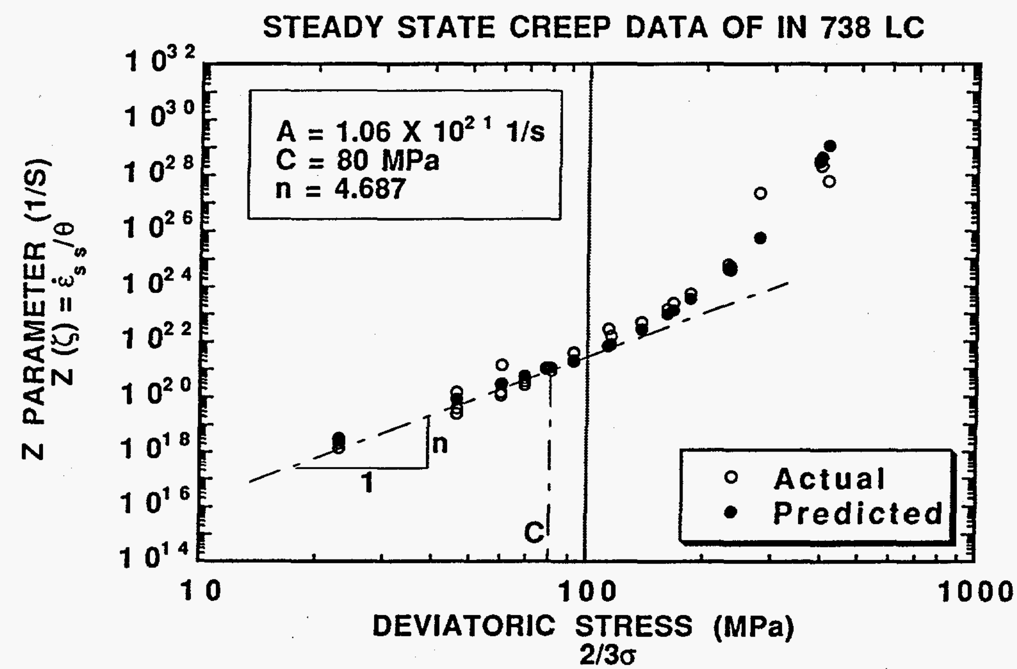

Figure 5. Zener-Hollomon plot of stress dependence of steady state creep rate illustrating determination of material parameter C

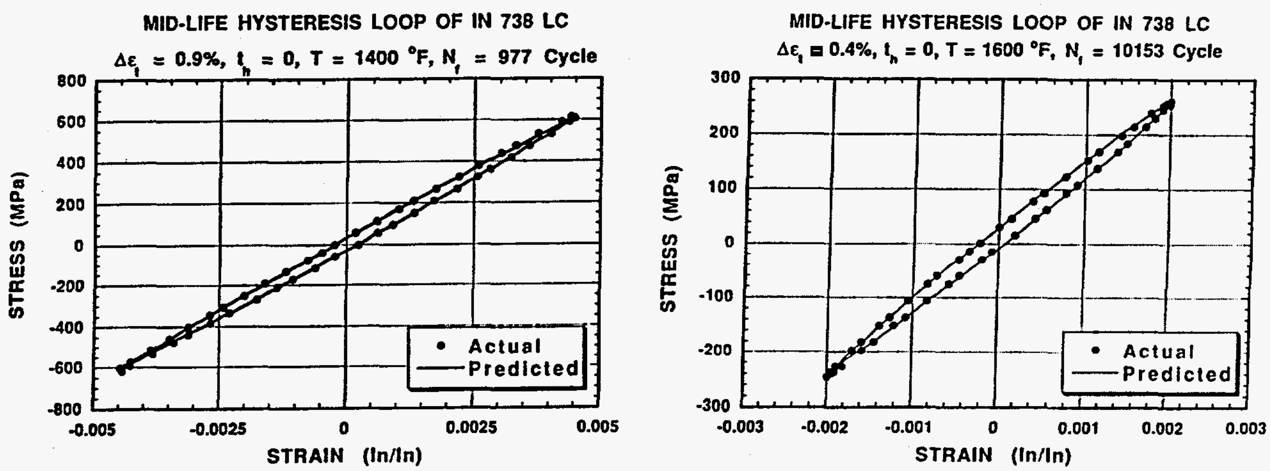

Figure 6. Predicted mid-life isothermal LCF hysteresis loops without hold time

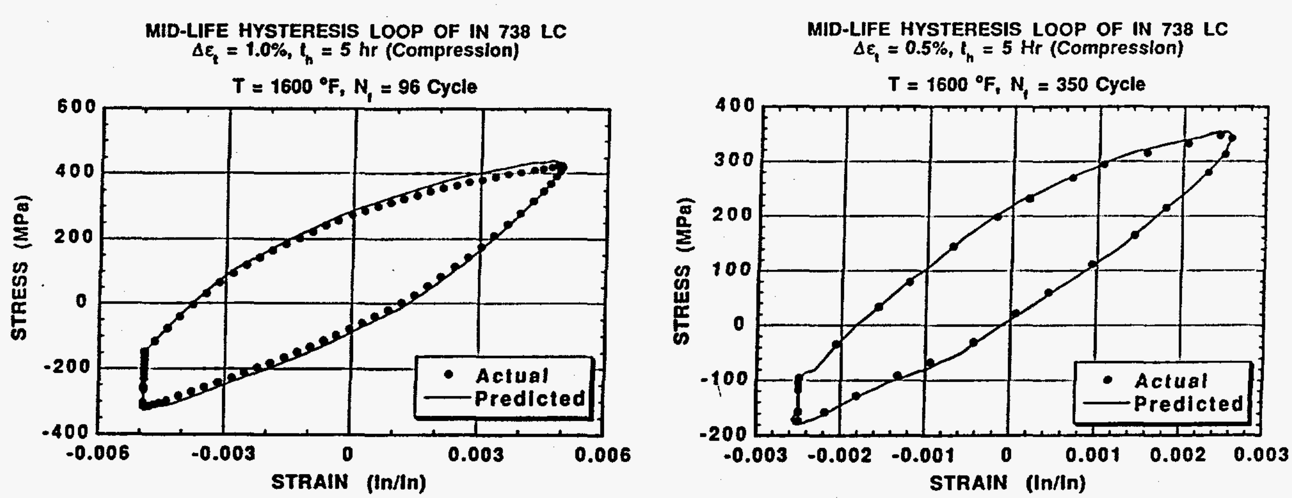

Figure 7. Predicted mid-life isothermal LCF hysteresis loops with hold time

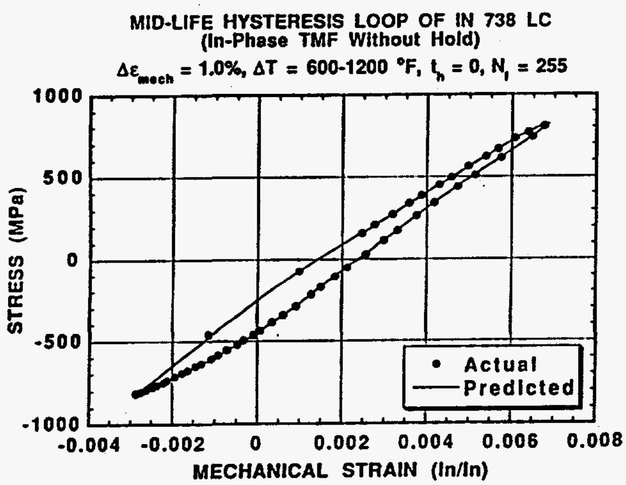

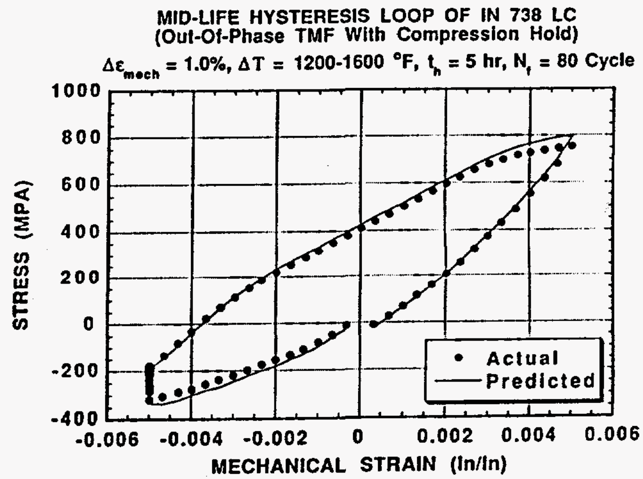

Figure 8. Predicted mid-life thermomechanical fatigue hysteresis loops

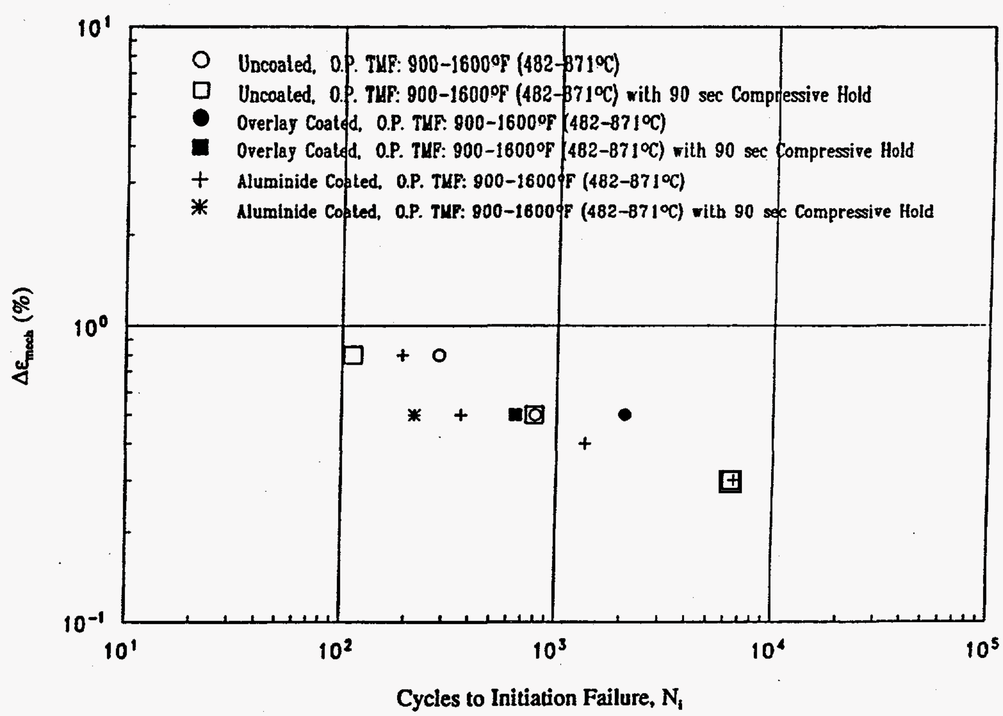

Figure 9. Penn State O.P. TMF Results

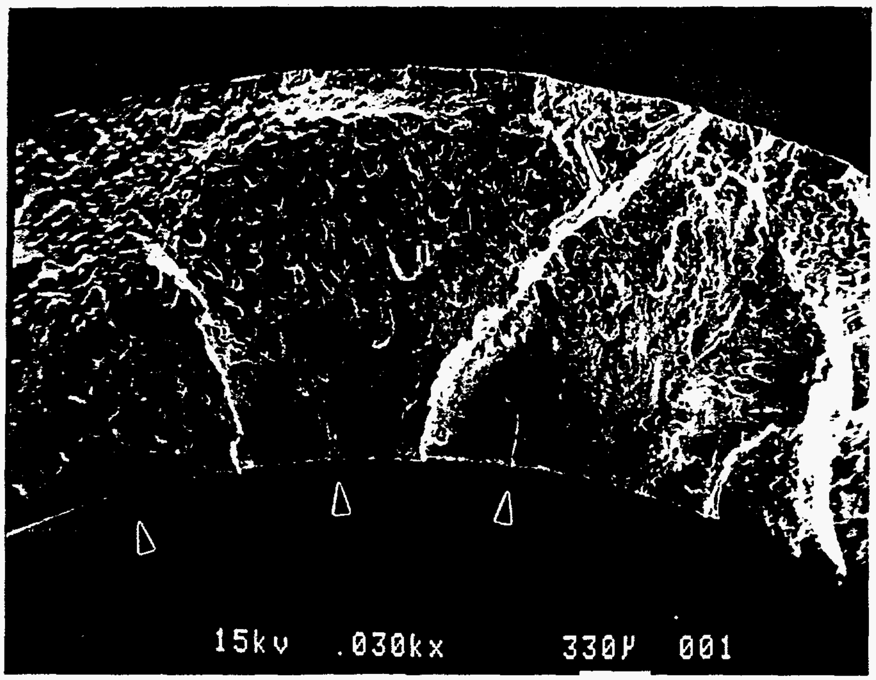

(a)

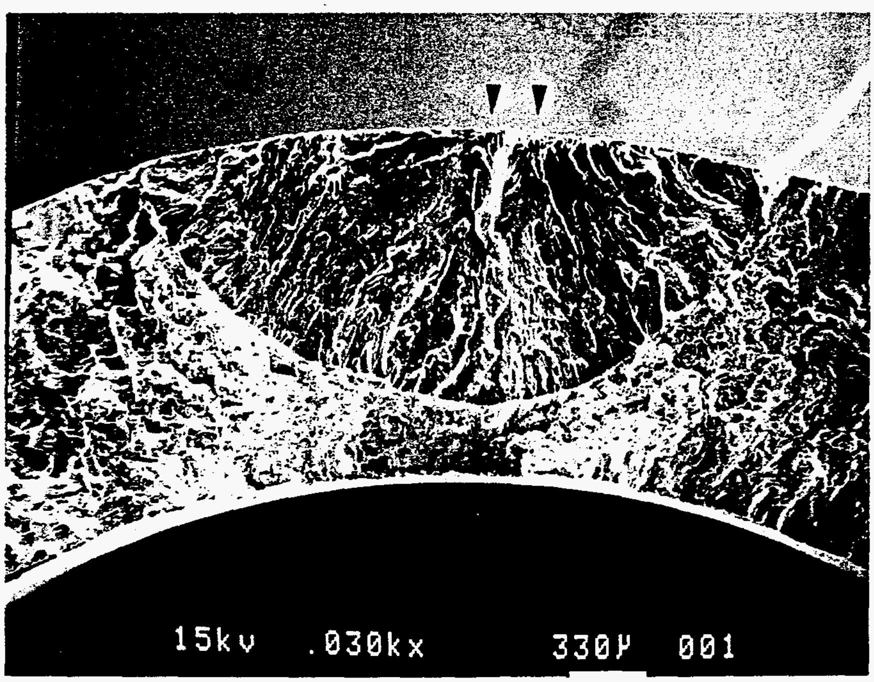

(b)

Figure 10. SEM fractographs of uncoated specimens showing: (a) interior wall fatigue crack initiations, $\Delta\varepsilon_{mech}$=0.5%, O.P. TMF, ΔT=900-500°F, N_i=5177 and (b) exterior wall fatigue crack initiation, $\Delta\varepsilon_{tot}$=0.5%, isothermal, T=1500°F, N_i=2494.

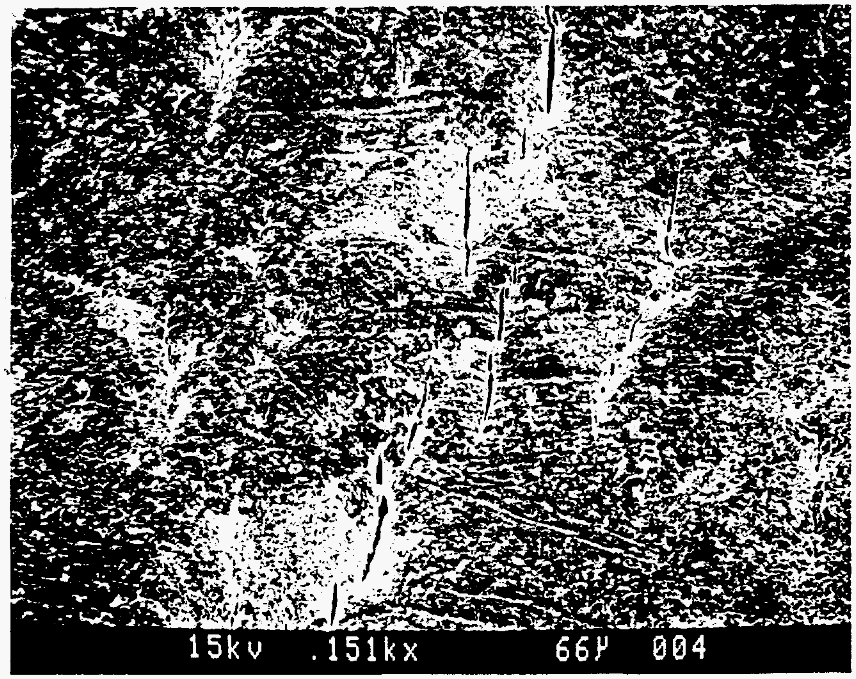

Figure 11. SEM micrograph showing surface fatigue cracks in overlay coating. $\Delta\varepsilon_{mech}$=0.5%, O.P. TMF, ΔT=900-1600°F, N_i=1171.

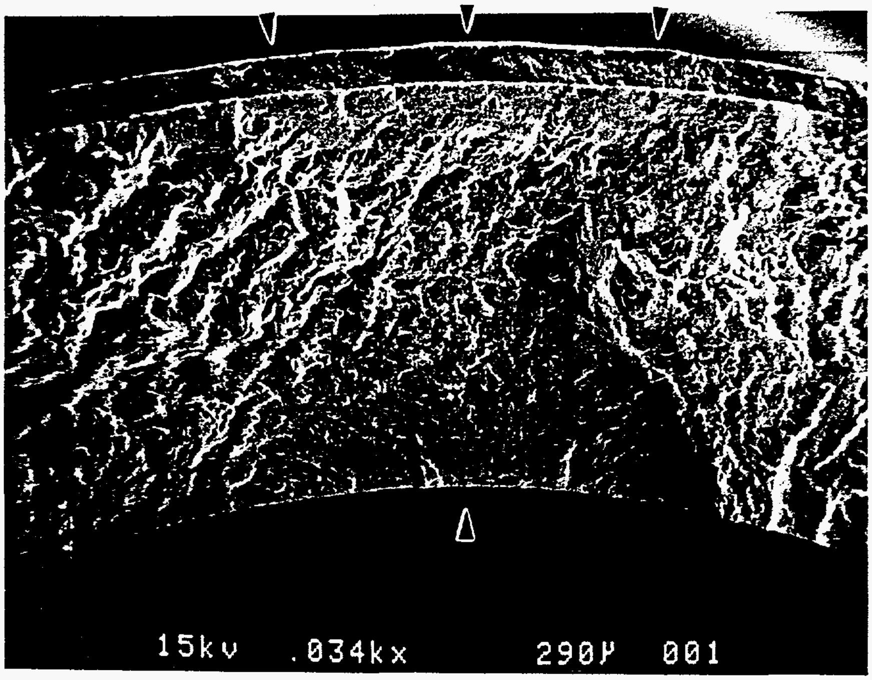

Figure 12. SEM fractograph showing fatal inner wall fatigue crack initiation and outer wall crack penetration through overlay coating and into substrate. $\Delta\varepsilon_{mech}$=0.5%, O.P. TMF, t_h=90 sec (comp), ΔT=900-600°F, N_i=643.

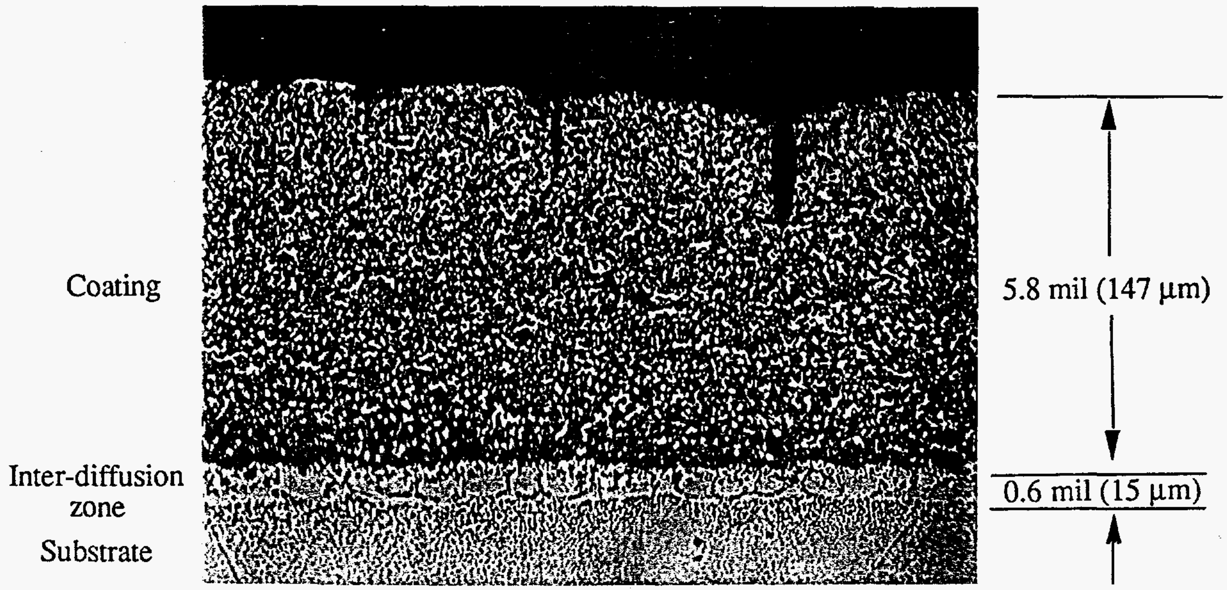

Figure 13. Crack initiation and blunting in overlay coating. $\Delta\varepsilon_{mech}$=0.5%, O.P. TMF, ΔT=900-1600°F, N_i=1171. (330X)

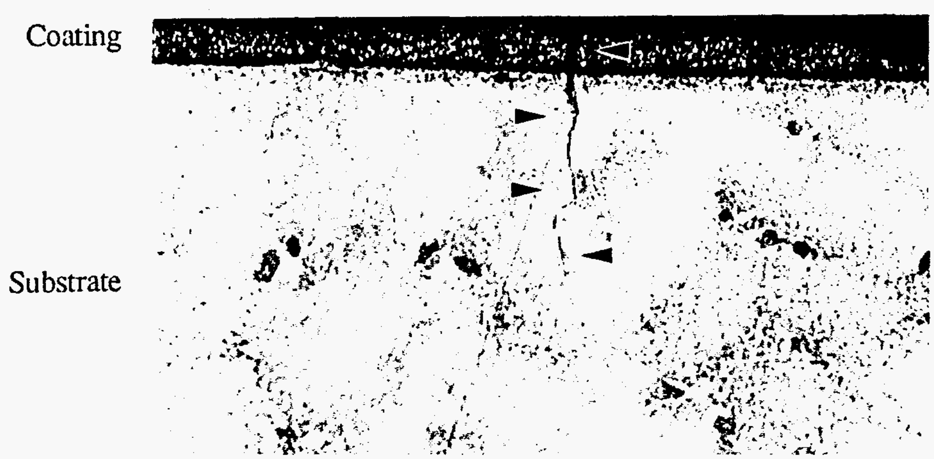

Figure 14. Light micrograph showing crack penetration through aluminide coating, inter-diffusion zone and substrate. $\Delta\varepsilon_{mech}$=0.5%, O.P. TMF, ΔT=900-1600°F, N_i=360. Crack length=7.6 mil (193 µm). (170 X)

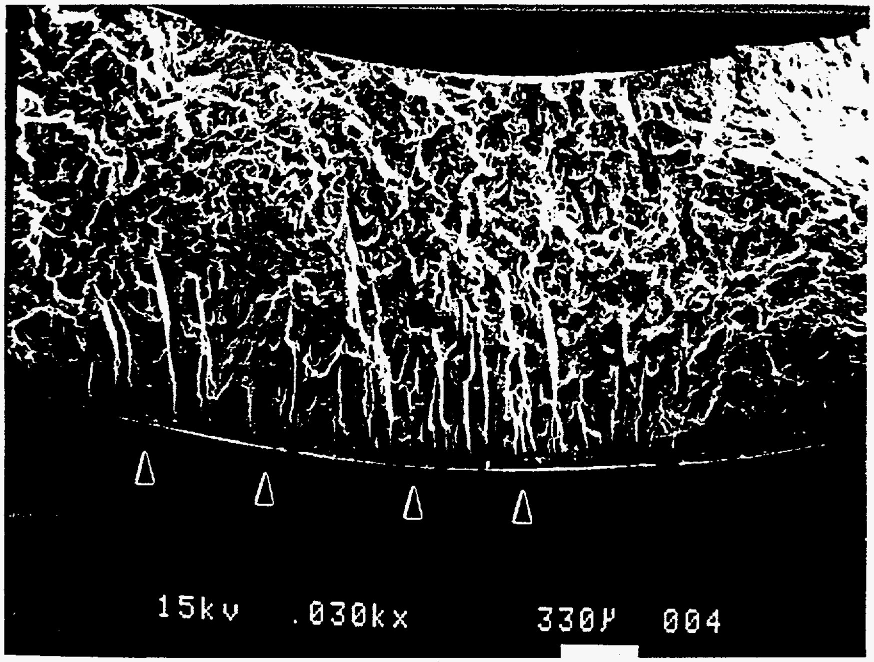

Figure 15. SEM fractograph showing numerous aluminide coating crack initiations. $\Delta\varepsilon_{mech}$=0.5%, O.P. TMF, ΔT=900-1600°F, N_i=360.

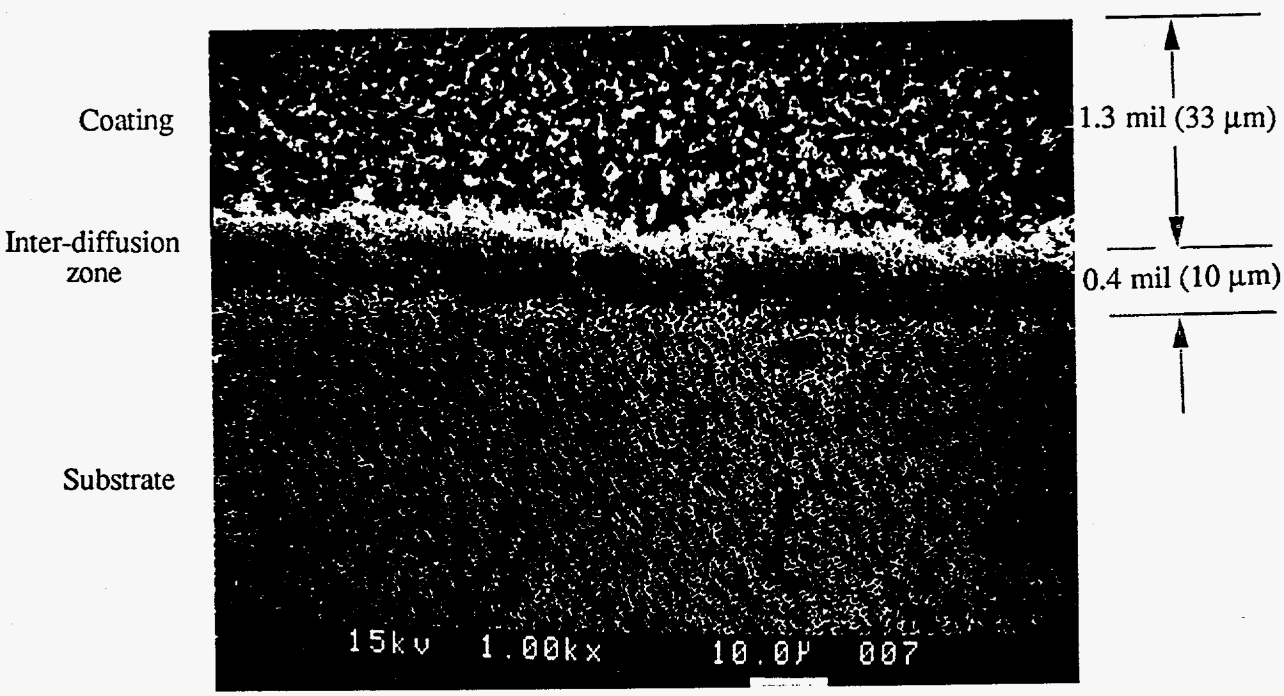

Figure 16. SEM micrograph showing etched coating and substrate microstructure after testing. $\Delta\varepsilon_{mech}$=0.5%, O.P. TMF, ΔT=900-600°F, N_i=360.